Applied Geochemistry 78 (2017) 83–95

Contents lists available at ScienceDirect

Applied Geochemistry

journal homepage: www.elsevier.com/locate/apgeochem

Uptake of arsenate by aluminum (hydr)oxide coated red scoria and pumice☆

Tsegaye Girma Asere [a, *], Jeriffa De Clercq [b], Kim Verbeken [c], Dejene A. Tessema [d], Fekadu Fufa [e], Christian V. Stevens [f], Gijs Du Laing [a]

[a] Laboratory of Analytical Chemistry and Applied Ecochemistry, Ghent University (UGent), Coupure Links 653, 9000 Ghent, Belgium
[b] Department of Chemical Engineering and Technical Chemistry, Ghent University (UGent), Valentin Vaerwyckweg 1, 9000 Ghent, Belgium
[c] Department of Materials Science and Engineering, Ghent University (UGent), Technologiepark 903, 9052 Zwijnaarde, Belgium
[d] Welkite University, Southern Nations, Nationalities and Peoples' Region, Welkite, Ethiopia
[e] Department of Water Resources and Environmental Engineering, Jimma University, P.O. Box 378, Jimma, Ethiopia
[f] Department of Sustainable Organic Chemistry and Technology, Ghent University (UGent), Coupure Links 653, 9000 Ghent, Belgium

ARTICLE INFO

Article history:
Received 21 July 2016
Received in revised form
18 December 2016
Accepted 21 December 2016
Available online 23 December 2016

Keywords:
Red scoria
Pumice
Aluminum
Arsenic
Adsorption

ABSTRACT

The development of cost effective and environmentally benign adsorbents for arsenic removal is absolutely required due to arsenic contamination of water sources in many regions around the globe. The use of materials which are locally available in the affected regions is important for successful implementation of the developed technologies in rural areas. In this regard, we treated volcanic rocks (red scoria and pumice) locally available in Ethiopia with an aluminum sulphate solution and evaluated these materials for their capacity to remove As(V) from aqueous systems. The adsorbents were characterized using ICP-OES, EDX, SEM and BET. The experimental sorption data fitted well a Freundlich isotherm and the pseudo-second-order model was found to be more suitable than the pseudo-first-order model to describe the adsorption kinetics. The Langmuir maximum adsorption capacity was 0.18 mg/g for aluminum-treated red scoria (Al-Rs) and 2.68 mg/g for aluminum-treated pumice (Al-Pu). The effect of pH, adsorbent dose, initial As(V) concentration and interfering ions on arsenic adsorption were studied. The leaching of aluminum from the adsorbent during the adsorption process was also investigated. Results of column experiments indicated that Al-Pu is suitable to treat low concentration of As(V) contaminated water. The Al-Pu adsorbent is recyclable with only about 9% loss of its original efficiency after the 3rd adsorption cycle (99.5%–90.2%). The data obtained from both batch and column studies indicate that Al-Rs and Al-Pu remove As(V) effectively from aqueous systems, with the latter being more efficient.

1. Introduction

Water is an essential natural resource supporting life and the environment, always having been considered to be present abundantly as a free gift of nature (Meenakshi and Maheshwari, 2006). Fast population growth, urbanization and industrialization, however, besides the deteriorating contamination status of the aqueous environment, have tremendously increased the demand for clean potable water (Ayoob et al., 2008). Hence, long ago one has begun to exploit groundwater resources for drinking and other domestic purposes. Regardless of the fact that aquifers are usually relatively safe from a microbiological point of view, various studies have indicated that groundwater sources in different regions across the world are chemically contaminated, and thus not safe for drinking (Bhutiani et al., 2016; Ehya and Marbouti, 2016; Lu et al., 2016; Rango et al., 2010). However, groundwater, which comprises about 97% of the global freshwater amount, is the main source of drinking water for more than half of the global population (Ayoob et al., 2008).

Elevated arsenic contents in water resources are a global problem because of the hazardous and carcinogenic nature of arsenic (Chen et al., 1992; Chiou et al., 1995; Tsai et al., 1999). The concentration of arsenic in natural water varies greatly depending on

☆ This paper has been recommended for acceptance by Prof. M. Kersten.

* Corresponding author. Department of Chemistry, Jimma University, P.O. Box 378, Jimma, Ethiopia.
E-mail address: tsegaye96@gmail.com (T.G. Asere).

http://dx.doi.org/10.1016/j.apgeochem.2016.12.013
0883-2927/

the local geology, hydrology and geochemical characteristics of the aquifer materials (Baskan and Pala, 2014). Arsenic mobilizes in the environment from natural pools, such as hot springs and mineral deposits. This can be facilitated by some human activities related to certain industries and mining. Arsenic contamination has been reported in about 105 countries affecting more than 226 million people worldwide (Pillewan et al., 2014). A high concentration of arsenic in drinking water has been reported in countries such as Argentina, Bangladesh, China, Chile, Canada, Hungary, India, Japan, Mexico, Poland, Taiwan, and USA (Danish et al., 2013).

Arsenic exists in water in different forms depending on the redox potential and pH of the medium, where the inorganic forms arsenite (As(III)) and arsenate (As(V)) are the most predominant species (Smedley and Kinniburgh, 2013). Arsenite is more toxic than arsenate (Pillewan et al., 2014; Styblo et al., 2000) due to the higher cellular uptake and the greater ability of arsenite to bind to sulfhydryl groups of proteins, as well as to form free radicals causing oxidative stress (Kitchin and Wallace, 2005; Neto et al., 2013; Tapio and Grosche, 2006). Exposure to the inorganic arsenic species is identified to be a risk for humans because it can affect lungs, skin, liver, kidney, and blood vessels (Chen et al., 1992; Chiou et al., 1995; Styblo et al., 2000; Tseng et al., 1996). For the sake of risk minimization of arsenic, the World Health Organization (WHO) has revised the permissible concentration of arsenic in drinking water from 50 to 10 μg/L (Organization; Smith and Smith, 2004; Zha et al., 2013). Therefore, highly effective and economical treatment processes for removing arsenic from aqueous systems are being developed by researchers aimed at meeting the stringent arsenic standard of the WHO. A moderate arsenic concentration, up to 190 μg/L, in the water bodies of the Main Ethiopian Rift Valley (MER) region was reported by Ahoule et al. (2015), where more than 80% of arsenic in the groundwater of this area exists as arsenate-As(V) (Rango et al., 2013).

Many different treatment techniques have been used in the removal of arsenic from aqueous systems. These methods include chemical precipitation, filtration, coagulation, anion exchange, reverse osmosis, adsorption techniques, and use of Donnan membranes (Tripathy and Raichur, 2008). Among them, adsorption processes appear to be the most promising because of the ease of handling, sludge-free operation, and the possibility of regeneration (Bhatnagar et al., 2011; Chen et al., 2010; Mohapatra et al., 2009). Moreover, the use of adsorbents which are locally available in the affected regions can help to reduce the cost and increase the technical feasibility and environmental sustainability of the developed technologies in rural areas. Various locally available natural adsorbent materials have been tested for the removal of arsenic by many researchers. However, the practical applicability of these natural adsorbents is limited either due to low efficiency, the need for pH adjustment, or dissolution problems (Fufa et al., 2014).

Coating and impregnation of natural adsorbents with some inorganic chemicals enhances their sorption capacity (Nasseri and Heidari, 2012; Salifu et al., 2013). For instance, aluminum oxide modified pumice was found to be effective for removal of fluoride from drinking water (Salifu et al., 2013). Far et al. (2012) showed that coating pumice with iron or manganese improves its As(V) adsorption capacity. Nasseri and Heidari (2012) also reported a higher As(V) removal efficiency of aluminum-coated zeolite compared to aluminum-coated pumice.

Pumice and scoria are the two most abundant volcanic rocks in areas with young volcanic fields. These rocks are abundant in many parts of the world including Ethiopia. The potential of volcanic rocks to remove both cationic and anionic ions from aqueous systems has been reported (Alemayehu and Lennartz, 2009, 2010; Alemayehu et al., 2011; Kwon et al., 2010). However, the preliminary tests in this study revealed that they exhibited poor As(V) adsorption. Therefore, the aim of this study was to prepare aluminum (hydr)oxide coated red scoria and pumice and evaluate their As(V) removal efficiency.

2. Materials and methods

2.1. Adsorbent preparation

2.1.1. Pumice and red scoria

The rock samples of red scoria and pumice were collected from volcanic cones of the Main Rift Valley, Ethiopia. The collected adsorbent samples were washed repeatedly with deionized water to remove any dust and water-soluble impurities. The rock samples were then dried at 55 °C for 48 h to evaporate the remaining water (Kwon et al., 2010; Sepehr et al., 2014). Then, the dried adsorbents were crushed in a mortar and sieved into four size fractions; i.e., silt (<0.075 mm), fine (0.075–0.425 mm), medium (0.425–2.0 mm), and coarse (2.0–4.75 mm) size following the American Society for Testing and Materials (ASTM D 422) soil textural classification system (Alemayehu and Lennartz, 2009; Liu and Evett, 2003). Then, the sieved samples were packed in air-tight plastic bags for later use.

2.1.2. Coating of aluminum (hydr)oxide onto red scoria and pumice

The coating of aluminum (hydr)oxide onto red scoria and pumice was carried out according to the method used by Salifu et al. (2013) with slight modification. An adequate amount of 0.5 M $Al_2(SO_4)_3$ was added to completely soak about 100 g of the dried red scoria (0.075–0.425 mm) in an Erlenmeyer flask. The mixture was shaken in an orbital shaker for 12 h at 200 rpm. Then, the red scoria was decanted and dried in an oven at 70 °C for 12 h. The dried red scoria was subsequently soaked in 5 M NH_4OH to neutralize it and complete the coating process. Then, the aluminum (hydr)oxide coated red scoria was drained and dried in an oven at 70 °C. The coated sample was washed several times with deionized water, dried at 70 °C for 48 h and stored for As(V) adsorption studies. The same procedure was used to prepare aluminum (hydr) oxide coated pumice.

2.2. Adsorbent characterization

2.2.1. Chemical composition

The elemental compositions of the geomaterials were analyzed using inductively coupled plasma optical emission spectrometry (ICP-OES, Varian Vista-MPX CCD Simultaneous ICP-OES). Total digestion of the samples was carried out using microwave digestion (Mars XP 1500Plus). The samples were treated with aqua regia and a hydrofluoric acid mixture in Teflon tubes, and then digested at a temperature of 250 °C and pressure of 200 psi. Then, the excess HF was neutralized using 4% boric acid. Subsequently, the elemental contents of both natural and aluminum (hydr)oxide coated pumice and red scoria samples were determined using ICP-OES. Energy dispersive x-ray (EDX) spectroscopy was employed to obtain information on the oxide content of the geomaterials. The surface morphology of both natural and Al-coated materials was determined using scanning electron microscope (FEG SEM JSM-7600F, JEOL, USA). The Brunauer–Emmett–Teller (BET) specific surface area of adsorbents was determined from N_2 gas adsorption/desorption isotherms obtained using BEL, Japan, Inc. Belsorp mini-II.

2.2.2. pH and point of zero charge

The pH of the natural and Al-coated adsorbents was measured using a pH meter in a 1:10 adsorbent: water suspension according to the standard method (Appel et al., 2003). The point of zero

charge (pH_{pzc}) of the adsorbents was determined in duplicate following a standard method using 0.01 M and 0.1 M solutions of NaCl as an electrolyte and adding 0.1 M solutions of NaOH or HCl (Karimaian et al., 2013; Sepehr et al., 2013).

2.2.3. Porosity

Porosity is a measure of the void spaces in a material, and is a measure of the volume of voids over the total volume. The porosity of pumice and red scoria was determined following the methods described in Sekomo et al. (2012).

2.3. Chemicals and reagents

All glassware and bottles were washed by 1% HNO_3 and rinsed with deionized water before use. A 1000 mg/L As(V) stock solution was prepared by dissolving an appropriate amount of $Na_2HAsO_4{\cdot}7H_2O$ (Merck KGaA, Darmstadt, Germany) in deionized water. Synthetic aqueous arsenic solutions for the adsorption experiments were prepared by diluting the stock solution with deionized water to obtain an arsenic concentration in the range of 0.1 mg/L – 25 mg/L. Solutions of bicarbonate, chloride, nitrate, sulfate and phosphate anions were prepared from their respective sodium salts.

2.4. Batch arsenic sorption studies

The batch adsorption experiments were performed in triplicate using 50 mL polyethylene plastic centrifuge tubes. A specific amount of dry adsorbent (Al-Rs or Al-Pu) was added to 25 mL of an arsenate solution having a desired pH value. The initial pH was adjusted using 0.1 M NaOH or 0.1 M HCl and afterwards the tubes were tightly closed. Then, the tubes were shaken at 200 rpm in a horizontal shaker at 25 °C for a predetermined period of time. The aqueous phase was filtered through a 0.45 μm membrane filter and the residual As(V) in the filtrate was measured using ICP-MS (ELAN DRC-e, PerkinElmer).

The As (V) adsorbent capacity, q_t (mg/g), at time t (min), and the As (V) removal efficiency (% adsorption) were determined using the equations (Eq. (1)) and (Eq. (2)), respectively.

$$q_t = (C_0 - C_t)\left(\frac{V}{W}\right) \tag{1}$$

$$\text{Adsorption}(\%) = \left(\frac{C_0 - C_t}{C_0}\right) \times 100 \tag{2}$$

where C_0 and C_t (mg/L) are the initial arsenic concentration and the concentration at time t (min), respectively, V is the solution volume (L) and W (g) is the adsorbent mass.

For the evaluation of the adsorption kinetics, 25 mL of 0.25 mg/L or 2.0 mg/L As(V) solution at pH 7.0 with 8 g/L (Al-Rs) and 5 g/L (Al-Pu) was used for a time period ranging from 0 to 9 h. Samples were taken at different contact times. The effect of adsorbent dose was studied by varying the adsorbent amounts from 0.1 to 25 g/L at fixed initial As(V) concentration of 0.25 mg/L at optimum time. The effect of initial pH on the adsorption process was studied by varying the solution pH from 3 to 12 at optimum time and adsorbent dose. To obtain the adsorption isotherms, experiments were conducted in batch using 25 mL As(V) solutions with concentrations ranging from 0.1 to 20 mg/L and an adsorbent dose of 8 g/L (Al-Rs) or 5 g/L (Al-Pu), adjusting the pH to 7.0 and shaking for 2 h (equilibration time). The effect of co-existing anions (Cl^-, NO_3^-, HCO_3^-, SO_4^{2-}, and PO_4^{3-}) on As(V) adsorption was also studied at fixed As(V) initial concentration of 0.25 mg/L and adsorbent dose of 8 g/L (Al-Rs) or 5 g/L (Al-Pu) while varying the anion concentration from 5 to 500 mg/L.

2.5. Regeneration of the adsorbents

Regeneration tests were carried out by using adsorbent Al-Rs or Al-Pu, which was previously loaded with 0.25 mg/L As(V) solution in a batch adsorption experiment. Then, the arsenic loaded adsorbents were subjected to desorption by adding 25 mL of 0.1 M NaOH solution in 50 mL centrifuge tubes and shaking the tubes at 200 rpm in a horizontal shaker for 2 h at 24 ± 1 °C. Subsequently, the suspensions were filtered and the arsenic content of the filtrate was measured. Afterwards, the adsorbents were soaked in dilute HCl (pH ~ 5.0–5.5). After rinsing with deionized water and drying at 70 °C for 24 h, the arsenic adsorption efficiency of the regenerated adsorbents was determined in a second adsorption cycle.

2.6. Column experiments

Column adsorption experiments were performed using a glass column with 1.0 cm internal diameter and a total length of 26 cm. Masses of 0.5 g, 1 g, and 3 g of the Al-Pu with corresponding bed heights of 1.25 cm, 2.5 cm, and 7.5 cm, respectively, were packed in the columns. Afterwards, the column was conditioned with deionized water and 0.25 mg/L of As(V) solution at pH 7.0 was passed through the column. The experiments were carried out in a down flow mode at a flow rate of 4.5 mL/min. Effluent samples were taken at predetermined time intervals and analyzed for arsenic and aluminum contents. The breakthrough point is identified as the number of bed volumes of treated water to reach the point where the effluent concentration exceeds 0.01 mg/L of As. The number of bed volumes (BV) is calculated as the ratio shown in Eq. (3).

$$BV = \frac{\text{Volume of the solution treated}}{\text{Volume of the adsorbent bed}} \tag{3}$$

2.7. Data analysis

2.7.1. Adsorption kinetics

Modeling the kinetic data is needed to predict the mechanism of adsorption and the potential rate-limiting steps. Therefore, pseudo-first-order, pseudo-second-order, and intraparticle diffusion models (Weber–Morris model) (Viswanathan et al., 2009) were used to analyze adsorption kinetics data. The nonlinear expressions of the pseudo-first-order, pseudo-second-order (Kumar, 2006), and intraparticle diffusion models are given in Eqs. (4)–(6), respectively.

$$q_t = q_e\left(1 - exp^{-K_1 t}\right) \tag{4}$$

$$q_t = \frac{k_2 q_e^2 t}{1 + k_2 q_e t} \tag{5}$$

$$q_t = k_p t^{0.5} + c \tag{6}$$

where, k_1 (min^{-1}) is pseudo-first-order rate constant, k_2 ($g\ mg^{-1}\ min^{-1}$) is pseudo-second-order rate constant, q_t and q_e are the arsenate adsorption capacity (mg/g) at any time t (min) and at equilibrium, respectively, k_p (mg/(g $min^{0.5}$) is the intraparticle diffusion rate constant; and c (mg/g) is the intercept of the intraparticle diffusion model. If the rate-limiting step of As(V) removal is the intraparticle diffusion, the plot of q_t against the $t^{1/2}$ should be a

straight line and pass through the origin (Pillewan et al., 2014).

2.7.2. Adsorption isotherms

Evaluation of experimental isotherm data is essential for designing an adsorption treatment system. Accordingly, the data were evaluated using three common isotherm models: Langmuir, Freundlich and Dubinin-Radushkevich (D-R) isotherm models. The Langmuir and the Freundlich isotherms are given in Eqs. (7) and (8), respectively.

$$q_e = \frac{Q_{max} b C_e}{(1 + bC_e)} \tag{7}$$

$$q_e = K_F C_e^{1/n} \tag{8}$$

where q_e (mg/g) is the equilibrium adsorption capacity of As(V); C_e (mg/L) is the equilibrium concentration of As(V) in the aqueous phase; Q_{max} (mg/g) is the maximum adsorption capacity based on the Langmuir equation; b (L/mg) is the Langmuir constant; K_F ($mg^{1-1/n}\ L^{1/n}/g$) is the adsorption coefficient based on the Freundlich equation; $^1/n$ is the adsorption intensity based on the Freundlich equation.

The D-R isotherm, given in Eq. (9) and Eq. (10), is used to evaluate the sorption energy and to understand the sorption mechanism of arsenic on aluminum coated volcanic rocks.

$$q_e = q_m \exp\left(-K_{DR}\varepsilon^2\right) \tag{9}$$

$$\varepsilon = RT \ln\left(1 + {}^1/C_e\right) \tag{10}$$

where q_e (mol/g) and q_m (mol/g) are the equilibrium adsorption capacity and the theoretical monolayer saturation capacity, respectively; K_{DR} (mol^2/kJ^2) is the activity coefficient related to the mean sorption energy; ε (mol^2/kJ^2) is the Polanyi potential; R (kJ/(mol. K)) is the gas constant; and T (K) is the temperature of the equilibrium experiment.

Besides the coefficient of determination, the nonlinear chi-square (χ^2) statistic test was used to identify the best model fit to the observed experimental data. The χ^2 is computed using Eq. (11) as described by Sundaram et al. (2008).

$$\chi^2 = \sum \frac{\left(q_e - q_{e,cal}\right)^2}{q_{e,cal}} \tag{11}$$

where $q_{e,cal}$ is the equilibrium adsorption capacity calculated from the model; and q_e is the experimental equilibrium adsorption capacity. A small χ^2 value indicates similarity of data between the modeled and the experimental data, whereas a larger χ^2 value implies variation between the modeled and experimental data (Sundaram et al., 2008).

3. Results and discussion

3.1. Adsorbent characterization

3.1.1. Chemical composition

Si, Al and Fe are the major elements in pumice and red scoria (Table 1) as determined by ICP-OES and confirmed by EDX. Other elements, except K (4%) in pumice and Ca (9.5%) in red scoria, were present in relatively smaller amounts or below the detection limit of the instrument. The EDX measurement indicated that the oxides of Si, Fe, and Al were the major constituents of both red scoria and pumice. Similar values were reported by Alemayehu and Lennartz (2009). Both the elemental and oxide compositions of the red scoria and pumice also indicate the absence of hazardous or carcinogenic substances. Therefore, they are considered appropriate as adsorbent to treat arsenic contaminated water.

The average aluminum contents of red scoria, pumice, Al-Rs and Al-Pu adsorbents were 103.5, 54.3, 108.3 and 64.6 mg Al/g, respectively. The net amount of aluminum coating onto the red scoria and pumice particles was thus 4.8 and 10.3 mg Al/g, respectively. Coating increased the aluminum (hydr)oxide contents of red scoria and pumice from 18.2% and 11.9% to 24.7% and 21.9%, respectively. The SEM pictures of red scoria and pumice before and after aluminum coating are shown in Fig. 1A–D. Apparent differences in morphology are observed between red scoria and pumice. The greater amount of aluminum (hydr)oxide loaded on pumice than red scoria may be due to the difference in porosity. The porosity of pumice (76.6%) was found to be much higher than red scoria (44.7%). The porosity of pumice can reach up to 90% (Asgari et al., 2012; Kitis et al., 2007). Alemayehu and Lennartz (2009) also mentioned the existence of a continuum (skeletal structure) pore space in pumice while the pore space of red scoria is dominated by dead-end pores. Hence, the aluminum sulphate solution may

Table 1
Elemental and oxide composition of red scoria (Rs), pumice (Pu), Al-Rs, and Al-Pu.

Element	Pu % (wt)	Rs % (wt)	Al-Pu % (wt)	Al-Rs % (wt)	Oxide	Pu oxide%	Rs oxide%	Al-Pu oxide%	Al-Rs oxide%
Si	27.2	18.4	25.5	19.3	SiO_2	68.7	44.5	62.8	42.3
Al	5.4	10.4	6.5	10.8	Al_2O_3	11.9	18.2	21.9	24.7
Fe	3.1	7.2	2.8	7.2	FeO	6.9	14.3	6.3	12.5
K	4.0	0.4	3.4	0.4	K_2O	6.6	0.6	5.1	0.5
Ca	0.4	9.5	0.1	9.5	CaO	0.9	11.3	0.6	10.6
Na	1.1	2.1	1.0	2.2	Na_2O	–	3.5	–	3.0
Mn	0.1	0.1	0.1	0.1	MnO	0.3	0.3	0.2	0.3
Mg	0.1	3.1	<0.1	2.9	MgO	0.2	4.9	–	3.5
Zn	<0.1	<0.1	<0.1	<0.1	ZnO	1.1	–	0.9	–
Ce	<0.1	<0.1	<0.1	<0.1	TiO_2	0.2	2.4	0.3	2.2
Cr	<0.1	<0.1	<0.1	<0.1	SO_3	0.1		0.8	0.6
Cu	<0.1	<0.1	<0.1	<0.1	CuO	1.7		0.9	
Co	<0.1	<0.1	<0.1	<0.1	NiO	1.3		–	
Cd	<0.1	<0.1	<0.1	<0.1					
Ni	<0.1	<0.1	<0.1	<0.1					
Pb	<0.1	<0.1	<0.1	<0.1					
As	<0.1	<0.1	<0.1	<0.1					

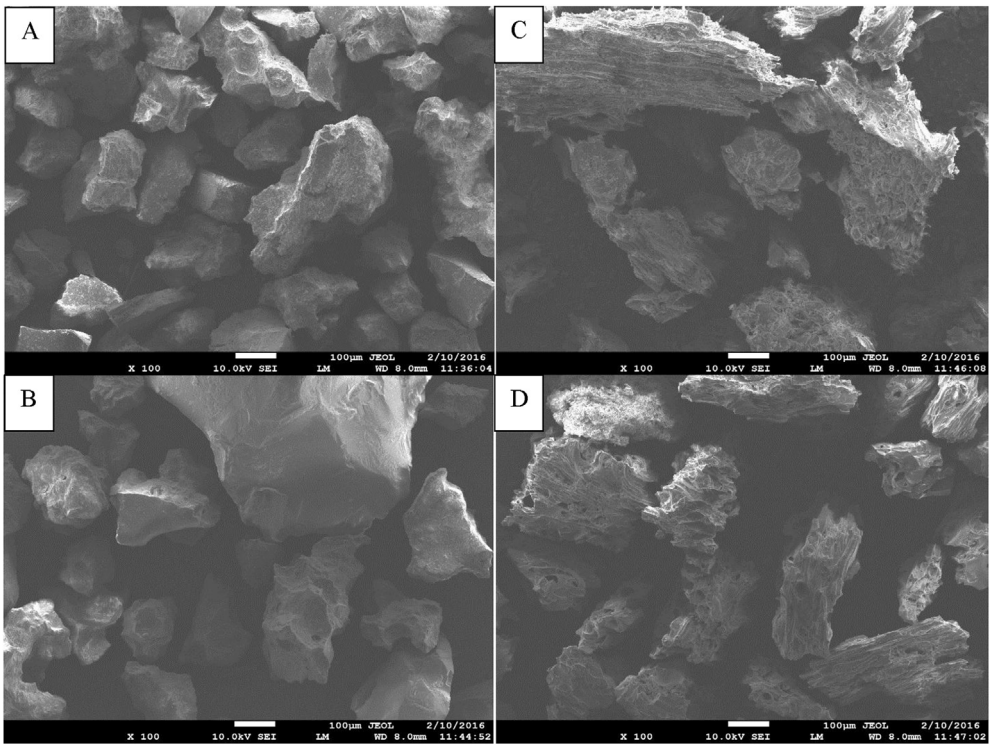

Fig. 1. SEM image of red scoria and pumice (fine particle size) with and without Aluminum coating: A) Rs, B) Al-Rs, C) Pu, and D) Al-Pu.

access all the pores of pumice compared to red scoria and coat the pumice with a much thin layer of aluminum (hydr)oxide than the red scoria. The difference in surface morphology was also confirmed by variation in specific surface area. The specific surface area of the red scoria, pumice, Al-Rs, and Al-Pu was 1.49, 2.82, 2.61, and 29.5 m^2/g, respectively. Coating with aluminum (hydr)oxide increased the specific surface area of pumice much more than red scoria. However, Salifu et al. (2013) reported that coating pumice with aluminum oxide decrease surface area of the pumice.

3.1.2. pH and point of zero charge

The pH of the adsorbents measured in water was found to be 9.38 (red scoria), 7.84 (pumice), 7.05 (Al-Rs), and 5.92 (Al-Pu), respectively. The point of zero charge (pH_{PZC}) for red scoria and pumice was 7.5 and 6.8, respectively, whereas the pH_{PZC} of Al-Rs and Al-Pu was 6.4 and 5.3, respectively. These shifts in pH_{PZC} can be attributed to a change in chemical characteristics of the surface as a result of coating with aluminum. Similar pH_{PZC} were reported for natural pumice by Sepehr et al. (2014) and aluminum-coated pumice by Salifu et al. (2013). It is known that the specific adsorption of anions by metal oxides shifts the PZC to lower pH values. Many anions such as HPO_4^{2-}, CO_3^{2-}, and SO_4^{2-} have been shown to produce this effect (Scholtz et al., 1985). The extent of shift varies depending on the nature of the metal oxide and the anionic species adsorbed. Therefore, the lower PZC of aluminum (hydr)oxide coated pumice and red scoria adsorbents may be due to the presence of some chemisorbed sulphate on the aluminum (hydr)oxide.

3.2. Sorption experiments

3.2.1. Adsorption kinetics

The adsorption kinetics of As(V) by Al-Rs and Al-Pu adsorbents are shown in Fig. 2. Rapid removal of As(V) by both adsorbents is observed at the early stage of adsorption. This could be due to external surface adsorption and availability of a lot of adsorption sites and smaller mass transfer resistance in the pores (Liu et al., 2013). During the first 5 min about 82.8% and 58.3% of As(V) is removed by Al-Pu (dose 5 g/L) and Al-Rs (dose 8 g/L), respectively, for 0.25 mg/L As(V) in the solution (Fig. 2A). This demonstrates that the As(V) adsorption onto Al-Rs is a slower process than that of Al-Pu. The next gradual adsorption stage may involve intraparticle diffusion which controls the adsorption rate up to the equilibrium point. Equilibrium was achieved after 45 min and 60 min for Al-Pu and Al-Rs, respectively, for 0.25 mg/L As(V) in the solution. However, to ensure maximum adsorption at equilibrium on the adsorbents, a contact time of 2 h was chosen for subsequent optimization of other adsorption parameters. At equilibrium, the amount of As(V) adsorbed onto Al-Rs and Al-Pu adsorbents was 0.036 mg/g (98.2%) and 0.053 mg/g (99.5%), respectively for 0.25 mg/L As(V) in the solution. The equilibrium time for Al-Pu was independent of the initial concentration (Fig. 2). However, Al-Rs required a longer time to reach equilibrium at higher As(V) concentration. The adsorption efficiency of Al-Rs was also lower at higher As(V) concentration compared to Al-Pu. This could be due to a greater amount of aluminum loaded on pumice than on red scoria.

The pseudo-first-order and pseudo-second-order arsenic adsorption kinetics fit is shown in Fig. 3A–D, and the values of k_1, k_2, $q_{e,cal}$ (calculated), and $q_{e,exp}$ (experimental) are presented in Table 2.

The values of $q_{e,cal}$ (calculated) and $q_{e,exp}$ (experimental) are similar for each adsorbent. The value of R^2 for the pseudo-first-order model was not satisfactory except for Al-Pu at lower (0.25 mg/L) initial As(V) concentration, but the pseudo-second-order kinetic model exhibited overall high R^2 and low χ^2 values (Table 2). Therefore, it can be concluded that the pseudo-second-order kinetic model is more suitable to describe the adsorption kinetics of arsenate on aluminum coated volcanic rocks (Al-Rs and Al-Pu).

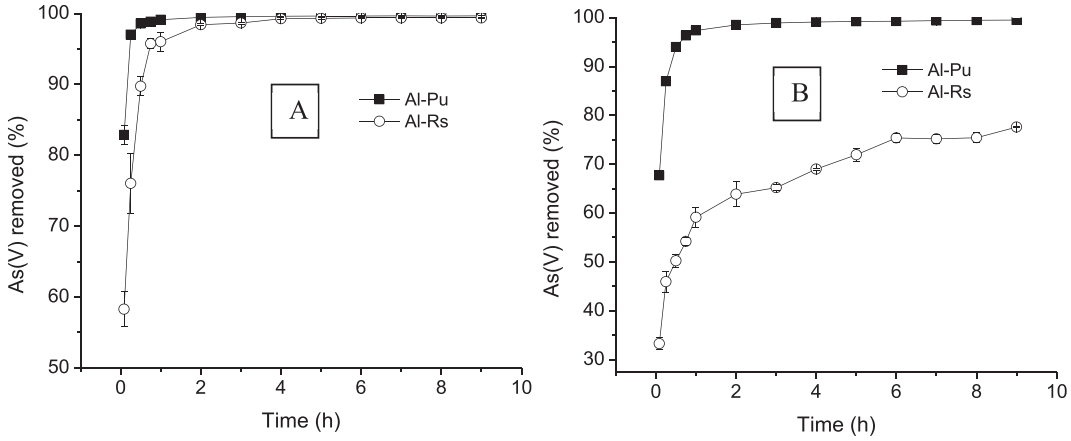

Fig. 2. Effect of contact time on removal of As(V) by Al-Rs (8 g/L dose) and Al-Pu (5 g/L)) at initial As(V) concentration of A) 0.25 mg/L and B) 2.0 mg/L (initial pH 7, shaking at 200 rpm at 24 ± 1 °C).

Table 2
Parameters of the pseudo-first-order and pseudo-second order kinetic models for As(V) adsorption on Al-Rs and Al-Pu.

Parameter	Al-Rs				Al-Pu			
	Pseudo-first-order		Pseudo-second-order		Pseudo-first-order		Pseudo-second-order	
Co(mg/L)	0.25	2.0	0.25	2.0	0.25	2.0	0.25	2.0
$q_{e,exp}$ (mg/g)	0.036	0.19	0.036	0.19	0.053	0.41	0.053	0.41
$q_{e,cal}$ (mg/g)	0.035	0.15	0.037	0.17	0.053	0.40	0.054	0.42
k_1 (min^{-1})	0.15	0.12	-	-	0.38	0.23	-	-
k_2 (g/(mg min))	-	-	6.75	0.98	-	-	20.22	0.99
V_0 (mg/(g min))	-	-	0.009	0.028	-	-	0.060	0.18
R^2	0.83775	0.6683	0.97731	0.8991	0.97439	0.90369	0.96016	0.99601
χ^2	4.66×10^{-6}	2.89×10^{-4}	6.52×10^{-7}	8.79×10^{-5}	2.03×10^{-7}	1.95×10^{-4}	3.16×10^{-7}	8.09×10^{-6}

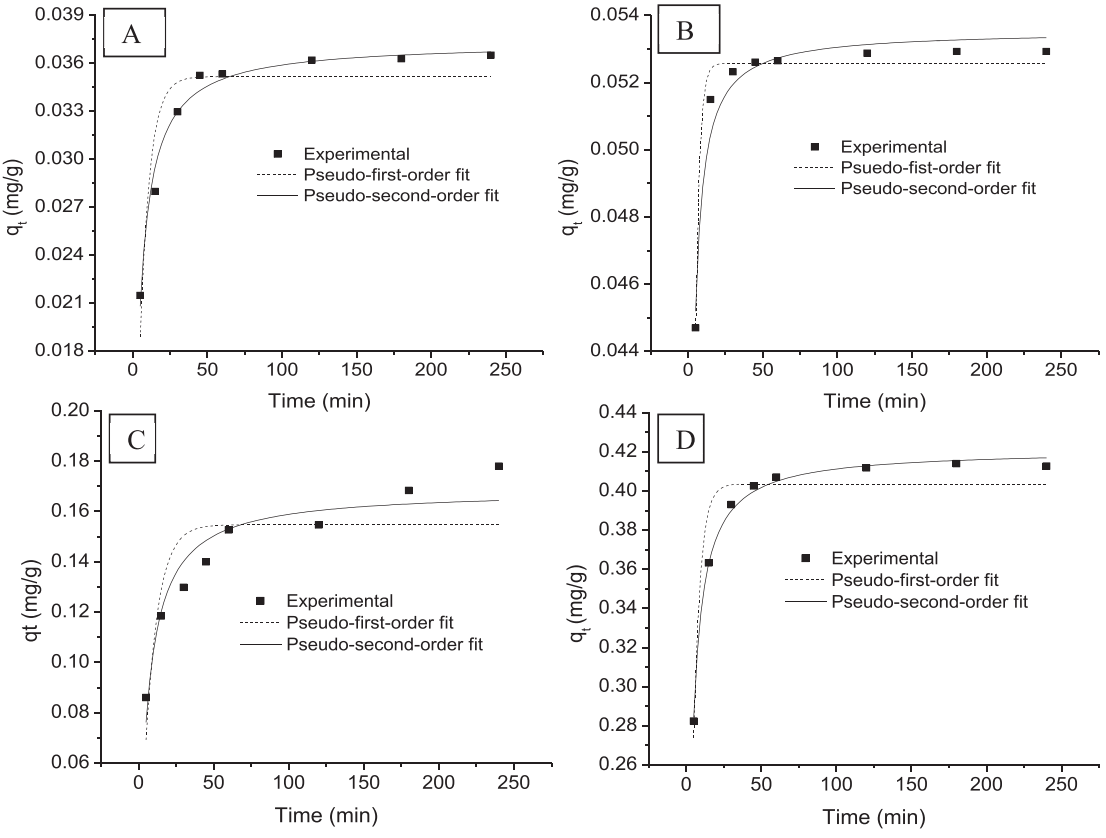

Fig. 3. Pseudo-first-order and pseudo-second-order kinetic model fits and experimental kinetic data: A) Al-Rs (8 g/L adsorbent and 0.25 mg/L As(V)), B) Al-Pu (5 g/L adsorbent and 0.25 mg/L As(V)), C) Al-Rs (8 g/L adsorbent and 2.0 mg/L As(V)), and D) Al-Pu (5 g/L adsorbent and 2.0 mg/L As(V)) (initial pH 7, shaking at 200 rpm at 24 ± 1 °C).

Adsorption affinity ($V_0 = K_2 q_e^2$) provides information on the adsorption rate at the beginning of the adsorption process. The calculated value of V_0 for Al-Rs and Al-Pu at both concentration levels indicates that the adsorption of Al-Pu was about 6.5 times faster than that of Al-Rs even at the lower dose of Al-Pu (5 g/L) compared to Al-Rs (8 g/L). However, the pseudo-second-order model has an inherent limitation by assuming the adsorption phenomenon as a single, one-step binding process, although the adsorption process proceeds in three steps, namely, external surface diffusion, intraparticle diffusion, and finally adsorption. Each of these steps could be rate-determining. Since the adsorption was carried out in a well-agitated system, external diffusion resistance could be quite small and intraparticle diffusion could be the rate-determining step. Therefore, the adsorption kinetics were examined by applying the Weber and Morris intraparticle diffusion model (Viswanathan et al., 2009) that is given by (Eq. (6)) in Section 2.7.1. Fig. 4 shows the results of experimental data fitted with the intraparticle diffusion model.

It is clear that each curve shows a multi-linear plot (Fig. 4A and B). However, each curve does not pass through the origin which indicates that intraparticle diffusion was not the only rate-determining step. Therefore, the adsorption of As(V) and its kinetics could be the overall effect of the external diffusion transport of As(V), the intraparticle diffusion of the ions and the adsorption of As(V) ions by the active sites on the adsorbent (Al-Rs and Al-Pu) (Fufa et al., 2014). In most of the previous studies, such as adsorption of As(V) onto aluminum oxide modified palygorskite (Zha et al., 2013), arsenate onto termite mound (Fufa et al., 2014), alum-impregnated activated alumina (Tripathy and Raichur, 2008) the plots did not pass through the origin and the intraparticle diffusion was not the only rate-controlling step.

3.2.2. *Effect of pH on As(V) removal and the adsorption mechanism*

The effect of pH on As(V) adsorption was investigated over a pH range of 3–12, keeping other parameters such as contact time, adsorbent dose and initial As(V) concentration constant. The As(V) removal by Al-Rs and Al-Pu at different initial solution pH levels is shown in Fig. 5A and B. Both Al-Rs and Al-Pu demonstrated remarkable adsorption efficiency in a wide range of pH levels from 3 to 10, which could avoid the need for pH adjustment in real applications. High As(V) adsorption in a wide pH range was also observed in previous studies using aluminum oxide modified palygorskite (Zha et al., 2013) and aluminum-coated pumice and zeolite (Nasseri and Heidari, 2012).

More than 98% of As(V) was removed by Al-Rs over the pH range of 5–9, leaving a maximum concentration of 0.0048 mg/L arsenic in the aqueous phase. Similarly, Al-Pu adsorbed about 99.5% of As(V) from water containing 0.25 mg/L As(V) in the pH range of 3–10, leaving about 0.0017 mg/L of arsenic in the treated water. Accordingly, both Al-Rs and Al-Pu are effective for treating arsenic contaminated water (~0.25 mg/L of As (V)) to the level below the WHO threshold (0.01 mg/L). The leaching of aluminum from both Al-Rs and Al-Pu adsorbents was negligible (<0.04 mg/L, the detection limit of ICP-OES and much lower than the WHO guideline of Al in drinking water (0.2 mg/L)) in the pH range of 5–9, indicating that no secondary pollution will be induced during treatments. Based on this observation, pH 7.0 ± 0.1 was chosen for the optimization of other adsorption parameters.

Adsorption dropped significantly at higher pH values (>10) and less than 20% adsorption occurred at pH 12. Similar trend was observed in earlier studies such as adsorption of As(V) on alum-impregnated activated alumina (Tripathy and Raichur, 2008), aluminum-coated pumice and zeolite (Nasseri and Heidari, 2012) and termite mound (Fufa et al., 2014). The observed decrease of As(V) uptake when the pH increases above 10 is most likely due to Coulomb repulsion between the negatively charged adsorbent surface and arsenate ions and/or competition for adsorption sites between arsenate ions and hydroxyl ions (Nasseri and Heidari, 2012). The high As(V) removal over a wide pH range could be ascribed to the pH buffering effect of aluminum oxides on the surfaces of the adsorbents (Fufa et al., 2014). The measured equilibrium pH levels varied in the range of 4.7–7.0 and 5.0–6.0 for Al-Rs and Al-Pu, respectively, when the initial pH levels of the solution varied between 4 and 9. The amphoteric nature of aluminum oxide could lower the equilibrium pH of the solution when the initial solution pH is in the alkaline region. The observed larger buffering effect of Al-Pu may be due to the higher amount of Al-oxide loading on pumice as compared to red scoria.

The aluminum oxide on the surface of dry adsorbents, when in contact with water, results in the formation of surface hydroxyl groups. The surface hydroxyl ions interact with positively charged aluminum to generate active surface sites called alumino groups (AlOH). At a pH below the pH_{pzc} of Al-Rs (6.4) and Al-Pu (5.3), the surface is positively charged. Arsenate mainly exists in the form of $H_2AsO_4^-$ and $HAsO_4^{2-}$ in the pH range of 3–11 (Tripathy and Raichur, 2008), which are the major species being adsorbed on the surface of Al-Rs and Al-Pu adsorbents. However, all the Al-OH-sites could not be positively charged at a pH below pH_{ZPC} Therefore, when the equilibrium pH of the solution is below pH_{pzc} of the adsorbents, the removal mechanism could be Coulomb attraction of arsenate

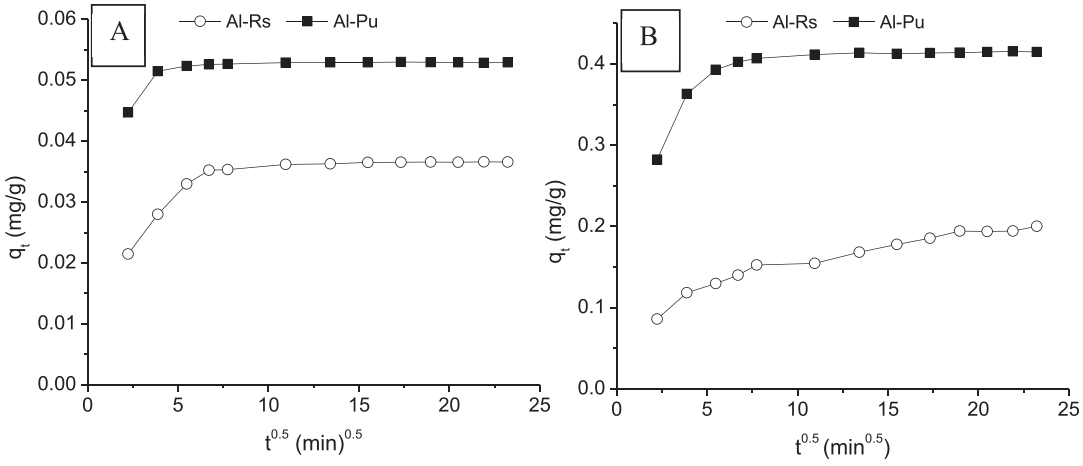

Fig. 4. Intraparticle diffusion plots of As(V) adsorption on Al-RS and Al-Pu at initial As(V) concentration of A) 0.25 mg/L and B) 2.0 mg/L.

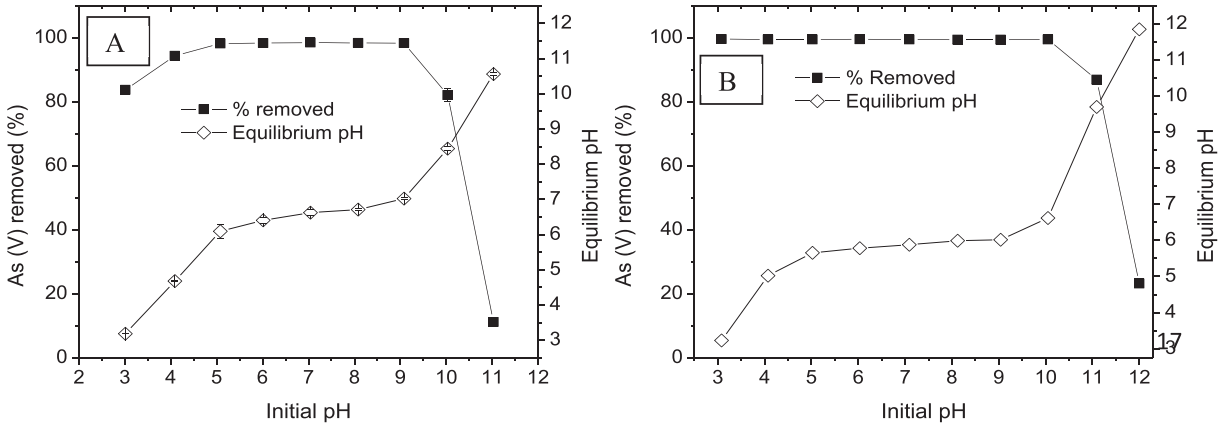

Fig. 5. Effect of initial pH on removal of As(V) by A) Al-Rs (8 g/L dose) and B) Al-Pu (5 g/L dose) (initial As(V) concentration 0.25 mg/L, shaking for 2 h at 200 rpm at 24 ± 1 °C).

anions by the positively charged surfaces (Eqs. (12)–(14)) and/or ligand exchange (Eqs. (15) and (16)):

$$\equiv AlOH + H^+ \leftrightarrow \equiv AlOH_2^+ \quad (12)$$

$$\equiv AlOH_2^+ + H_2AsO_4^- \leftrightarrow \equiv AlOH_2 - - - H_2AsO_4 \quad (13)$$

$$\equiv (AlOH_2^+)_2 + HAsO_4^{2-} \leftrightarrow \equiv (AlOH_2)_2 - - - HAsO_4 \quad (14)$$

where AlOH and $AlOH_2^+$ are the neutral and protonated sites on Al-Rs and Al-Pu, respectively.

It was also noted that when the equilibrium pH is higher than the pH_{pzc} of Al-Rs (6.4) and Al-Pu (5.3), a significant amount of As(V) is removed by both adsorbents. At equilibrium pH between 6.4 and 8.4, 82% to 98% of As(V) was removed by Al-Rs. Similarly, 87% to 99% of As(V) was removed by Al-Pu when the equilibrium pH was between 5.4 and 9.7. This indicates that the arsenate ions were most probably removed by the following ligand exchange reactions at a pH higher than the pH_{pzc} of the adsorbents (D'Arcy et al., 2011; Nigussie et al., 2007):

$$\equiv Al\text{-}OH + H_2AsO_4^- \leftrightarrow \equiv Al\text{-}H_2AsO_4 + OH^- \quad (15)$$

$$\equiv Al\text{-}OH + HAsO_4^{2-} \leftrightarrow \equiv Al\text{-}HAsO_4^- + OH^- \quad (16)$$

3.2.3. Effect of adsorbent dose

The adsorbent dosage is another important factor affecting the adsorption process. Experiments were performed using different masses of the adsorbents (1–25 g/L) and 0.25 mg/L As(V) concentration. The As(V) removal efficiency increased from 67.9% to 98.2% (Al-Rs) and 95.3% to 99.5% (Al-Pu) as the dose varied from 1 g/L to 8 g/L (Al-Rs) and from 1 g/L to 5 g/L (Al-Pu), and slightly thereafter (Fig. 6A and B). The increase in adsorption efficiency with increase of the adsorbent dose is due to the greater availability of active surface sites for arsenate binding at a higher adsorbent dose (Salifu et al., 2013). However, the increase of removal efficiency was found to be negligible above an adsorbent dose of 8 g/L (Al-Rs) and 5 g/L (Al-Pu), which thus may be considered the optimum dose. Dosages of 8 g/L Al-Rs and 5 g/L Al-Pu were found to lower an arsenic concentration of 0.25 mg/L to below the WHO guideline value (0.01 mg/L) of drinking water. On the other hand, the amount of As(V) adsorbed per unit mass of adsorbent, q_e (mg/g), decreased from 0.17 mg/g to 0.01 mg/g (Al-Rs) and from 0.26 mg/g to 0.01 mg/g (Al-Pu) with increasing adsorbent doses from 1 g/L to 25 g/L for the fixed As(V) concentration (Fig. 6A and B). The decrease in adsorbed amount with increase in adsorbent dose for a fixed As(V) concentration was possibly due to the lower ratio of As(V) ions to the available active binding sites with increase in dose, i.e. fewer As(V) ions were available per unit mass of adsorbent (Thole, 2011).

3.2.4. Adsorption isotherm

The Langmuir, Freundlich and D-R isotherm equations are given

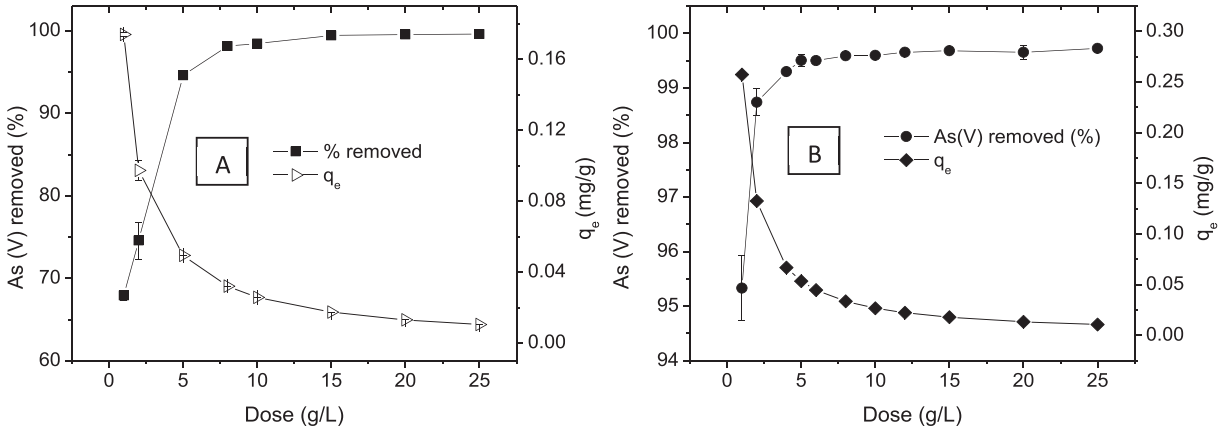

Fig. 6. Effect of adsorbent dose on removal of As(V) by A) Al-Rs and B) Al-Pu (0.25 mg/L initial As(V) concentration, pH 7, shaking for 2 h at 200 rpm at 24 ± 1 °C).

in Eqs. (7)–(9) (section 2.7.2). The isotherm plots for As(V) adsorption on Al-Rs and Al-Pu are graphically presented in Fig. 7A–D. The values of the different isotherm parameters are given in Table 3.

The experimental data of Al-Rs and Al-Pu fitted well to both the Langmuir and Freundlich isotherms. The Langmuir isotherm gives a maximum adsorption capacity of 0.18 mg/g and 2.68 mg/g for Al-Rs and Al-Pu, respectively. The separation factor (R_L), computed using the relation $R_L = 1/(1 + bC_0)$, is used to predict the nature of the adsorption process (Gupta and Ghosh, 2009). The adsorption process is irreversible if $R_L = 0$, favorable if $0 < R_L < 1$, linear if $R_L = 1$ and unfavorable if $R_L > 1$. The obtained values of R_L are within the range 0–1 (Table 3), suggesting favorable equilibrium adsorption of As(V) on both Al-Rs and Al-Pu (Gupta and Ghosh, 2009). Table 4 presents a summary of reported maximum adsorption capacities of some natural and modified adsorbents aimed at evaluating the effectiveness of Al-Pu and Al-Rs adsorbents. This evaluation indicated generally a good maximum adsorption capacity of arsenate onto the Al-Pu and Al-Rs adsorbents when compared to several the other adsorbents (Table 4). However, compared to some hybrid oxides such as iron-manganese and cerium-titanium binary oxides, the adsorption capacity of the Al-Pu and Al-Rs adsorbents was low. Even though the adsorption capacity of the materials is low, they have several advantages from an economic point of view: pumice and red scoria are widely available in many countries such as Italy, Turkey, Spain, Ethiopia, and Kenya. The $Al_2(SO_4)_3$ is not costly and also locally produced even in Ethiopia. The Al-Pu and Al-Rs have showed very good removal of low arsenate concentrations from water. The potential to reuse the adsorbents, particularly Al-Pu, is also an advantage improving the commercial viability of the adsorbents.

In the Freundlich isotherm, the 1/n value is closely related to surface heterogeneity and ranges between 0 and 1 when the

Table 3
Langmuir, Freundlich and D-R isotherm parameters of the adsorption of As(V) on Al-Rs and Al-Pu.

Isotherm	Parameters	Al-Rs	Al-Pu
Langmuir	q_{max} (mg/g)	0.182	2.678
	b (L/mg)	16.843	2.630
	R_L	0.010–0.352	0.019–0.752
	R^2	0.942	0.970
	χ^2	2.74×10^{-4}	2.73×10^{-2}
Freundlich	$K_F((mg^{1-1/n}L^{1/n})/g)$	0.150	1.599
	n	4.678	3.039
	R^2	0.958	0.982
	χ^2	1.97×10^{-4}	1.64×10^{-2}
D-R	q_m (mol/g)	1.78×10^{-5}	1.27×10^{-4}
	K_{DR} (mol^2/KJ^2)	3.39×10^{-3}	2.25×10^{-3}
	E_{DR} (KJ/mol)	12.145	14.907
	R^2	0.939	0.995
	χ^2	5.11×10^{-14}	7.89×10^{-13}

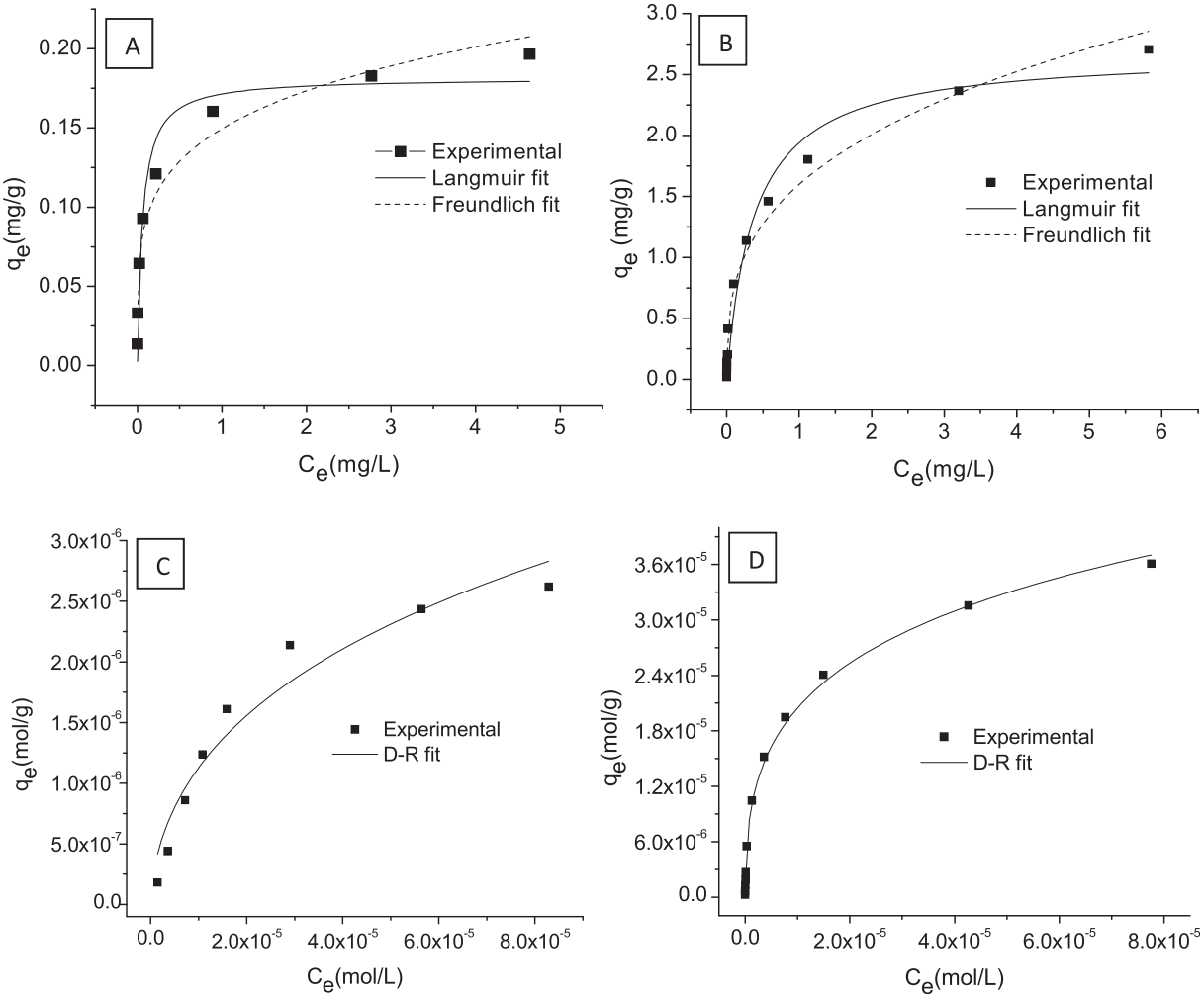

Fig. 7. Langmuir, Freundlich and D-R isotherm plots of equilibrium adsorption of As(V) on Al-Rs (A and C) and Al-Pu (B and D).

Table 4
Maximum adsorption capacities of some adsorbents for As(V) adsorption.

Adsorbent	pH	Adsorbent dose (g/L)	As(V) conc. (mg/L)	Adsorption capacity (mg/g)	References
Feldspar	3	8	0.2–15	0.235	Yazdani et al. (2016)
Iron oxide impregnated activated carbon	2.6	20	1–50	1.208	Lee et al. (2016)
Manganese oxide coated zeolite	7	10	0.1–3	0.151	Massoudinejad et al. (2015)
Natural iron ores	4.5–6.5	5	0–30	0.4	Zhang et al. (2004)
Iron-manganese binary oxide	4.8	0.2	0.5–50	72	Zhang et al. (2007)
Cerium-titanium binary oxide	6.5	0.1	0.02–20	49.9	Li et al. (2010)
Akadama mud	3	10	5–100	5.3	Chen et al. (2010)
Iron coated pottery granules	7		5–100	1.74	Dong et al. (2009)
Iron-oxide coated sands		24	0.01–0.5	0.021	Hsu et al. (2008)
Kaolinite, montmorillonite and illite		40	10–200	0.86, 0.64, and 0.52, respectively	Mohapatra et al. (2007)
Al-Rs	7	8	0.1–6.3	0.18	This study
Al-Pu	7	5	0.1–20	2.68	This study

adsorption is favorable (He et al., 2015). The value of K_F for Al-Pu (1.60) is about 10 times that of Al-Rs (0.15), indicating the higher affinity of As(V) for Al-Pu than Al-Rs (Table 3) which is consistent with the conclusions drawn from the kinetic data (section 3.2.1).

The D–R isotherm model assumes that the ionic species bind preferentially to the most energetically favorable adsorption sites and allows for multilayer sorption of ions (Boyaci et al., 2010). The mean sorption energy, E_{DR} (kJ/mol), of equilibrium As(V) adsorption was computed from the D-R isotherm using the equation $E_{DR} = (2K_{DR})^{-0.5}$ (Gupta and Ghosh, 2009). The K_{DR}, provides information about the mean free energy of sorption, defined as the energy required to transfer one mole of ions to the surface of the solid from infinity in the solution (Boyaci et al., 2010). The E_{DR} value of an adsorption system is used to predict the mechanism of the adsorption process of a solute on an adsorbent. The adsorption process is physical if $0 < E_{DR} < 8$ kJ/mol, and considered to be chemical if 8 kJ/mol $< E_{DR} <$ 16 kJ/mol (Fufa et al., 2013). In the present study, the values of E_{DR} computed for the equilibrium adsorption of As(V) on Al-Rs and Al-Pu were 12.15 kJ/mol and 14.91 kJ/mol, respectively. Accordingly, chemisorption plays a significant role in the removal of As(V) by Al-Rs and Al-Pu which is consistent with the proposed ligand exchange mechanism in section 3.2.2.

3.2.5. Effect of co-existing anions

Anions that exist in the natural aquatic environment and polluted waters can compete with As(V) for active sites of the adsorbent, thereby, hindering the removal of arsenic. To investigate the effect of interfering ions on removal of As(V) by Al-Rs and Al-Pu, adsorption experiments were carried out in the presence of 10 mg/L, 50 mg/L, 100 mg/L, 250 mg/L and 500 mg/L salt solutions of chloride (Cl^-), nitrate (NO_3^-), bicarbonate (HCO_3^-), sulphate (SO_4^{2-}) and phosphate (PO_4^{3-}), separately and in a mixture (Fufa et al., 2014). The arsenic removal efficiency of the adsorbents in presence of interfering anions is given in Fig. 8A and B. Cl^- and NO_3^- ions up to 500 mg/L concentrations have no significant effect on As(V) removal by Al-Rs. HCO_3^- at a concentration higher than 100 mg/L hinders considerably the removal of As(V) by Al-Rs. Presence of phosphate causes a significant decrease of As(V) removal by both Al-Rs and Al-Pu due to the powerful competitive adsorption between phosphate and arsenate for active sites. This results from the analogous structure and similar charge properties of phosphate and arsenate species. However, phosphate is absent or very rarely occurs at high concentrations in the groundwater, so its effect on As(V) removal should not be a problem in real applications (Alemayehu, 2004; McKenzie et al., 2001). Anions up to 500 mg/L of Cl^-, SO_4^{2-}, NO_3^- separately, had no considerable effect on removal of As(V) by Al-Pu. The observed reduction in adsorption of As(V) due the presence of interfering anions was in the order of $PO_4^{3-} \gg HCO_3^- > SO_4^{2-} > NO_3^- \cong Cl^-$.

3.2.6. Desorption and regeneration

The reusable nature of adsorbents is a key feature required in developing cost-effective and environmentally benign adsorbents

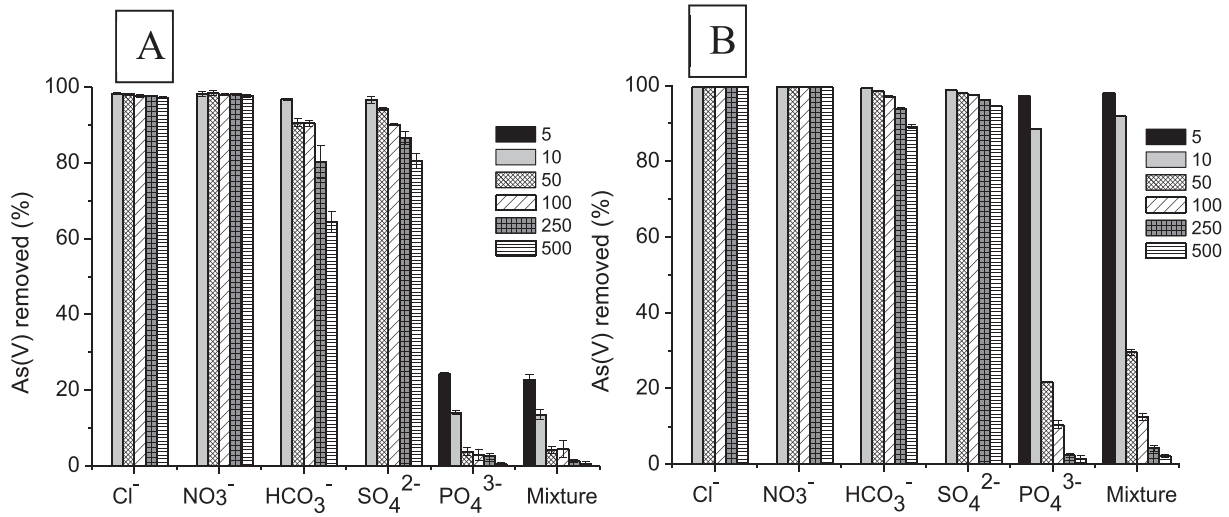

Fig. 8. Effect of co-existing anions on As(V) removal by A) Al-Rs (8 g/L dose) and B) Al-Pu (5 g/L dose) (As(V) initial concentration 0.25 mg/L, pH 7, shaking at 200 rpm for 2 h, at 24 ± 1 °C).

for pollutant removal from aqueous systems. In the present study, desorption experiments were carried out with loaded adsorbents of Al-Rs and Al-Pu which showed poor adsorption at a pH above 10. Therefore, desorption tests were conducted using 0.1 M NaOH solution. The reusability of Al-Rs and Al-Pu is presented in Fig. 9. The regeneration studies were carried out up to the 2nd and 4th cycles for Al-Rs and Al-Pu, respectively. The removal efficiency of Al-Rs dropped from 98.5% to 59.3% in the second cycle while for Al-Pu the loss in efficiency was only about 9% even for the 3rd adsorption cycle (99.5–90.2). Moreover, the maximum aluminum leaching during the adsorption process was found to be 0.06 mg/L and 0.11 mg/L for Al-Pu and Al-Rs, respectively which is below the WHO guideline of Al (0.2 mg/L) in drinking water. This indicates that the aluminum oxide coated volcanic rocks are efficient for As(V) removal from aqueous systems.

3.2.7. Column studies

A preliminary column study was performed using Al-Pu by passing a feed concentration of 0.25 mg/L As(V) at a flow rate of 4.5 mL/min. A plot of C/Co versus time is shown in Fig. 10, where C is the effluent concentration and Co is the influent concentration (0.25 mg/L). The breakthrough point (= WHO standard of 0.01 mg/L As) occurred at about 1222, 2050 and 3558 bed volumes for the bed heights of 1.25 cm, 2.5 cm, and 7.5 cm, respectively. Service times were found to be 4.3, 15.4, and 76.2 h for 1.25, 2.5, and 7.5 cm bed heights, respectively. A higher As(V) uptake was observed at higher bed height due to the increased amount of adsorbent which provided more active binding sites for adsorptions of the arsenate ions. Increase in bed volume and service time as bed height increases was also observed in most of the previous studies (Danish et al., 2013; Liu et al., 2014; Saha and Sarkar, 2016).

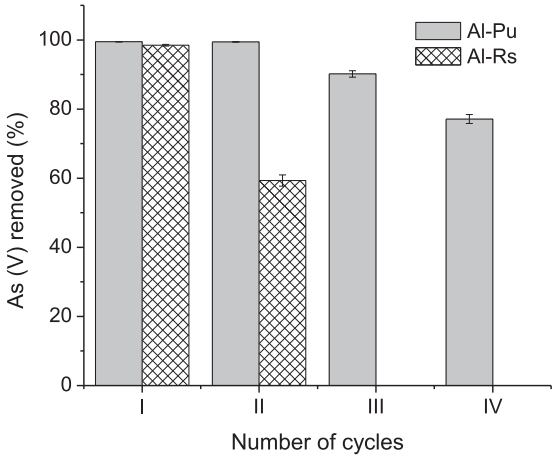

Fig. 9. As(V) removed by Al-Rs and Al-Pu in different adsorption cycles following different desorption cycles.

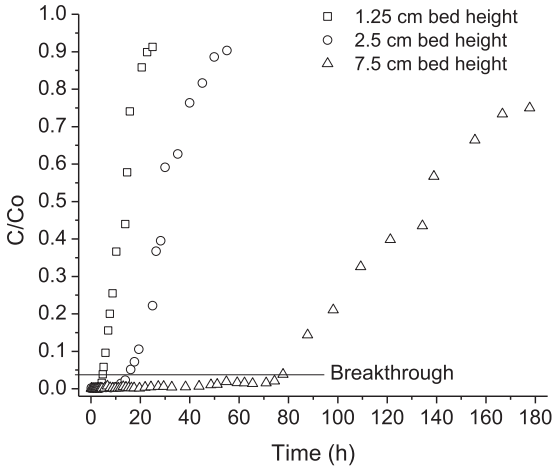

Fig. 10. Breakthrough curves of As(V) adsorption on Al-Pu loaded in columns having different bed heights at initial As(V) concentration of 0.25 mg/L, pH 7, and flow rate of 4.5 mL/min.

4. Conclusion

Both Al-Rs and Al-Pu adsorbents can remove As(V) from aqueous systems. They exhibit remarkable As(V) removal efficiency in a pH range between 3 and 10 which may be due to the pH buffering effect of aluminum oxides coated on the surfaces of the adsorbents. The adsorption is very fast and reaches equilibrium within 45 and 60 min for Al-Pu and Al-Rs, respectively. The kinetic data fit well to the pseudo-second-order model. Al-Pu (5 g/L) can lower an arsenic concentration of 1.028 mg/L to levels below the WHO guideline (<0.01 mg/L) for drinking water, whereas Al-Rs (8 g/L) could treat a maximum of 0.270 mg/L As(V) solution to the level below the WHO guideline. The Langmuir maximum adsorption capacity (q_{max}) of Al-Pu (2.68 mg/g) is higher than that of Al-Rs (0.18 mg/g) which could be due to the greater amount of aluminum oxide coated on pumice than red scoria. The D-R model predicts adsorption of As(V) on both Al-Rs and Al-Pu surfaces to be a chemisorption process. The high As(V) removal efficiency of both adsorbents above their corresponding pH_{pzc} values indicate the possibility of ligand exchange reactions. Other anions, except phosphate, had a negligible interfering effect in the treatment of As(V) using Al-Rs and Al-Pu. The Al-Pu adsorbent can be recycled and used up to three adsorption cycles without significant loss in efficiency. The Al-Pu adsorbent packed in a column with 1.0 cm internal diameter could also treat a 0.25 mg/L As(V) solution of 1222 BV, 2050 BV and 3558 BV for bed heights 1.25 cm, 2.5 cm, and 7.5 cm, respectively. Therefore, both the batch and column results suggest the suitability of Al-Pu for removal of arsenic from As(V) contaminated water. Further evaluation of the adsorbents for removal of arsenic in groundwater in field is required to demonstrate that they could be promising for practical drinking water treatment.

Acknowledgements

The first author would like to thank Gent University, Belgium, for financial support of this researcher through a Special Research Fund fellowship (Scholarship code: 01W05414). We are grateful to Elien Wallaert, Department of Materials Science and Engineering, Gent University, Belgium for SEM and EDX measurements. The authors are also thankful to Tom Planckaert and Karen Leus, Department of Inorganic and Physical Chemistry, Ghent University, Belgium for BET analysis of the adsorbents.

References

Ahoule, D.G., Lalanne, F., Mendret, J., Brosillon, S., Maiga, A.H., 2015. Arsenic in African waters: a review. Water Air Soil Pollut. 226.
Alemayehu, T., 2004. Water pollution by natural inorganic chemicals in the central part of the Main Ethiopian Rift. SINET Ethiop. J. Sci. 23, 197–214.
Alemayehu, E., Lennartz, B., 2009. Virgin volcanic rocks: kinetics and equilibrium studies for the adsorption of cadmium from water. J. Hazard. Mater. 169, 395–401.
Alemayehu, E., Lennartz, B., 2010. Adsorptive removal of nickel from water using volcanic rocks. Appl. Geochem. 25, 1596–1602.
Alemayehu, E., Thiele-Bruhn, S., Lennartz, B., 2011. Adsorption behaviour of Cr(VI)

onto macro and micro-vesicular volcanic rocks from water. Sep. Purif. Technol. 78, 55–61.
Appel, C., Ma, L.Q., Rhue, R.D., Kennelley, E., 2003. Point of zero charge determination in soils and minerals via traditional methods and detection of electroacoustic mobility. Geoderma 113, 77–93.
Asgari, G., Roshani, B., Ghanizadeh, G., 2012. The investigation of kinetic and isotherm of fluoride adsorption onto functionalize pumice stone. J. Hazard. Mater. 217–218, 123–132.
Ayoob, S., Gupta, A.K., Bhat, V.T., 2008. A conceptual overview on sustainable technologies for the defluoridation of drinking water. Crit. Rev. Environ. Sci. Technol. 38, 401–470.
Baskan, M.B., Pala, A., 2014. Batch and fixed-bed column studies of arsenic adsorption on the natural and modified clinoptilolite. Water Air Soil Pollut. 225.
Bhatnagar, A., Kumar, E., Sillanpaa, M., 2011. Fluoride removal from water by adsorption-A review. Chem. Eng. J. 171, 811–840.
Bhutiani, R., Kulkarni, D.B., Khanna, D.R., Gautam, A., 2016. Water quality, pollution source apportionment and Health risk assessment of heavy metals in groundwater of an industrial area in North India. Expo. Health 8, 3–18.
Boyaci, E., Eroglu, A.E., Shahwan, T., 2010. Sorption of As(V) from waters using chitosan and chitosan-immobilized sodium silicate prior to atomic spectrometric determination. Talanta 80, 1452–1460.
Chen, C.J., Chen, C.W., Wu, M.M., Kuo, T.L., 1992. Cancer potential in liver, lung, bladder and kidney due to ingested inorganic arsenic in drinking water. Br. J. Cancer 66, 888–892.
Chen, R., Zhang, Z., Feng, C., Lei, Z., Li, Y., Li, M., Shimizu, K., Sugiura, N., 2010. Batch study of arsenate (V) adsorption using Akadama mud: effect of water mineralization. Appl. Surf. Sci. 256, 2961–2967.
Chiou, H.-Y., Hsueh, Y.-M., Liaw, K.-F., Horng, S.-F., Chiang, M.-H., Pu, Y.-S., Lin, J.S.-N., Huang, C.-H., Chen, C.-J., 1995. Incidence of internal cancers and ingested inorganic arsenic: a seven-year follow-up study in Taiwan. Cancer Res. 55, 1296–1300.
Danish, M.I., Qazi, I.A., Zeb, A., Habib, A., Awan, M.A., Khan, Z., 2013. Arsenic removal from aqueous solution using pure and metal-doped titania nanoparticles coated on glass beads: adsorption and column studies. J. Nanomater. 2013, 1–17. Article No. 69.
Dong, L., Zinin, P.V., Cowen, J.P., Ming, L.C., 2009. Iron coated pottery granules for arsenic removal from drinking water. J. Hazard. Mater. 168, 626–632.
D'Arcy, M., Weiss, D., Bluck, M., Vilar, R., 2011. Adsorption kinetics, capacity and mechanism of arsenate and phosphate on a bifunctional TiO_2–Fe_2O_3 bi-composite. J. Colloid Interface Sci. 364, 205–212.
Ehya, F., Marbouti, Z., 2016. Hydrochemistry and contamination of groundwater resources in the Behbahan plain, SW Iran. Environ. Earth Sci. 75.
Far, L.B., Souri, B., Heidari, M., Khoshnavazi, R., 2012. Evaluation of iron and manganese-coated pumice application for the removal of As (v) from aqueous solutions. Iran. J. Environ. Health Sci. Eng. 9, 1.
Fufa, F., Alemayehu, E., Lennartz, B., 2013. Defluoridation of groundwater using termite mound. Water Air Soil Pollut. 224, 1552.
Fufa, F., Alemayehu, E., Lennartz, B., 2014. Sorptive removal of arsenate using termite mound. J. Environ. Manag. 132, 188–196.
Gupta, K., Ghosh, U.C., 2009. Arsenic removal using hydrous nanostructure iron(-III)–titanium(IV) binary mixed oxide from aqueous solution. J. Hazard. Mater. 161, 884–892.
He, S.F., Han, C.Y., Wang, H., Zhu, W.J., He, S.Y., He, D.D., Luo, Y.M., 2015. Uptake of Arsenic(V) using alumina functionalized highly ordered mesoporous SBA-15 (Al-x-SBA-15) as an effective adsorbent. J. Chem. Eng. Data 60, 1300–1310.
Hsu, J.C., Lin, C.J., Liao, C.H., Chen, S.T., 2008. Removal of As(V) and As(III) by reclaimed iron-oxide coated sands. J. Hazard. Mater. 153, 817–826.
Karimaian, K.A., Amrane, A., Kazemian, H., Panahi, R., Zarrabi, M., 2013. Retention of phosphorous ions on natural and engineered waste pumice: characterization, equilibrium, competing ions, regeneration, kinetic, equilibrium and thermodynamic study. Appl. Surf. Sci. 284, 419–431.
Kitchin, K.T., Wallace, K., 2005. Arsenite binding to synthetic peptides based on the Zn finger region and the estrogen binding region of the human estrogen receptor-α. Toxicol. Appl. Pharmacol. 206, 66–72.
Kitis, M., Kaplan, S.S., Karakaya, E., Yigit, N.O., Civelekoglu, G., 2007. Adsorption of natural organic matter from waters by iron coated pumice. Chemosphere 66, 130–138.
Kumar, K.V., 2006. Linear and non-linear regression analysis for the sorption kinetics of methylene blue onto activated carbon. J. Hazard. Mater. 137, 1538–1544.
Kwon, J.S., Yun, S.T., Lee, J.H., Kim, S.O., Jo, H.Y., 2010. Removal of divalent heavy metals (Cd, Cu, Pb, and Zn) and arsenic(III) from aqueous solutions using scoria: kinetics and equilibria of sorption. J. Hazard. Mater. 174, 307–313.
Lee, I., Park, J.A., Kim, J.H., Kang, J.K., Lee, C.G., Kim, S.B., 2016. Functionalization of activated carbon fiber through iron oxide impregnation for As(V) removal: equilibrium, kinetic, and thermodynamic analyses. Desalin. Water Treat. 57, 10757–10766.
Li, Z.J., Deng, S.B., Yu, G., Huang, J., Lim, V.C., 2010. As(V) and As(III) removal from water by a Ce-Ti oxide adsorbent: behavior and mechanism. Chem. Eng. J. 161, 106–113.
Liu, C., Evett, J., 2003. Soil Properties—testing, Measurement, and Evaluation. Banta Book Company, USA, ISBN 0-13-093005-9.
Liu, B., Wang, D., Yu, G., Meng, X., 2013. Removal of F- from aqueous solution using Zr(IV) impregnated dithiocarbamate modified chitosan beads. Chem. Eng. J. 228, 224–231.
Liu, J., Huang, X., Liu, J., Wang, W., Zhang, W., Dong, F., 2014. Adsorption of arsenic (V) on bone char: batch, column and modeling studies. Environ. Earth Sci. 72, 2081–2090.
Lu, Y.T., Tang, C.Y., Chen, J.Y., Yao, H., 2016. Assessment of major ions and heavy metals in groundwater: a case study from Guangzhou and Zhuhai of the Pearl River Delta, China. Front. Earth Sci. 10, 340–351.
Massoudinejad, M., Asadi, A., Vosoughi, M., Gholami, M., Karami, M.A., 2015. A comprehensive study (kinetic, thermodynamic and equilibrium) of arsenic (V) adsorption using KMnO4 modified clinoptilolite. Korean J. Chem. Eng. 32, 2078–2086.
McKenzie, J.M., Siegel, D.I., Patterson, W., McKenzie, D.J., 2001. A geochemical survey of spring water from the main Ethiopian rift valley, southern Ethiopia: implications for well-head protection. Hydrogeol. J. 9, 265–272.
Meenakshi, Maheshwari, R.C., 2006. Fluoride in drinking water and its removal. J. Hazard. Mater. 137, 456–463.
Mohapatra, D., Mishra, D., Chaudhury, G.R., Das, R.P., 2007. Arsenic(V) adsorption mechanism using kaolinite, montmorillonite and illite from aqueous medium. J. Environ. Sci. Health Part a-Toxic Hazard. Subst. Environ. Eng. 42, 463–469.
Mohapatra, M., Anand, S., Mishra, B.K., Giles, D.E., Singh, P., 2009. Review of fluoride removal from drinking water. J. Environ. Manag. 91, 67–77.
Nasseri, S., Heidari, M., 2012. Evaluation and comparison of aluminum-coated pumice and zeolite in arsenic removal from water resources. Iran. J. Environ. Health Sci. Eng. 9.
Neto, J.D.M., Bellato, C.R., Milagres, J.L., Pessoa, K.D., de Alvarenga, E.S., 2013. Preparation and evaluation of chitosan beads immobilized with iron(III) for the removal of As(III) and As(V) from water. J. Braz. Chem. Soc. 24, 121–132.
Nigussie, W., Zewge, F., Chandravanshi, B.S., 2007. Removal of excess fluoride from water using waste residue from alum manufacturing process. J. Hazard. Mater. 147, 954–963.
Pillewan, P., Mukherjee, S., Meher, A.K., Rayalu, S., Bansiwal, A., 2014. Removal of arsenic (III) and arsenic (V) using copper exchange zeolite-A. Environ. Prog. Sustain. Energy 33, 1274–1282.
Rango, T., Bianchini, G., Beccaluva, L., Tassinari, R., 2010. Geochemistry and water quality assessment of central Main Ethiopian Rift natural waters with emphasis on source and occurrence of fluoride and arsenic. J. Afr. Earth Sci. 57, 479–491.
Rango, T., Vengosh, A., Dwyer, G., Bianchini, G., 2013. Mobilization of arsenic and other naturally occurring contaminants in groundwater of the Main Ethiopian Rift aquifers. Water Res. 47, 5801–5818.
Saha, S., Sarkar, P., 2016. Arsenic mitigation by chitosan-based porous magnesia-impregnated alumina: performance evaluation in continuous packed bed column. Int. J. Environ. Sci. Technol. 13, 243–256.
Salifu, A., Petrusevski, B., Ghebremichael, K., Modestus, L., Buamah, R., Aubry, C., Amy, G.L., 2013. Aluminum (hydr)oxide coated pumice for fluoride removal from drinking water: synthesis, equilibrium, kinetics and mechanism. Chem. Eng. J. 228, 63–74.
Scholtz, E.C., Feldkamp, J.R., White, J.L., Hem, S.L., 1985. Point of zero charge of amorphous aluminum hydroxide as a function of adsorbed carbonate. J. Pharm. Sci. 74, 478–481.
Sekomo, C.B., Rousseau, D.P.L., Lens, P.N.L., 2012. Use of Gisenyi volcanic rock for adsorptive removal of Cd(II), Cu(II), Pb(II), and Zn(II) from wastewater. Water Air Soil Pollut. 223, 533–547.
Sepehr, M.N., Zarrabi, M., Kazemian, H., Amrane, A., Yaghmaian, K., Ghaffari, H.R., 2013. Removal of hardness agents, calcium and magnesium, by natural and alkaline modified pumice stones in single and binary systems. Appl. Surf. Sci. 274, 295–305.
Sepehr, M.N., Amrane, A., Karimaian, K.A., Zarrabi, M., Ghaffari, H.R., 2014. Potential of waste pumice and surface modified pumice for hexavalent chromium removal: characterization, equilibrium, thermodynamic and kinetic study. J. Taiwan Inst. Chem. Eng. 45, 635–647.
Smedley, P.L., Kinniburgh, D., 2013. Arsenic in groundwater and the environment. In: Selinus, O. (Ed.), Essentials of Medical Geology. Springer Netherlands, pp. 279–310.
Smith, A.H., Smith, M.M.H., 2004. Arsenic drinking water regulations in developing countries with extensive exposure. Toxicology 198, 39–44.
Styblo, M., Del Razo, L.M., Vega, L., Germolec, D.R., LeCluyse, E.L., Hamilton, G.A., Reed, W., Wang, C., Cullen, W.R., Thomas, D.J., 2000. Comparative toxicity of trivalent and pentavalent inorganic and methylated arsenicals in rat and human cells. Arch. Toxicol. 74, 289–299.
Sundaram, C.S., Viswanathan, N., Meenakshi, S., 2008. Defluoridation chemistry of synthetic hydroxyapatite at nano scale: equilibrium and kinetic studies. J. Hazard. Mater. 155, 206–215.
Tapio, S., Grosche, B., 2006. Arsenic in the aetiology of cancer. Mutat. Res Rev. Mutat. Res. 612, 215–246.
Thole, B., 2011. Defluoridation kinetics of 200 °C calcined bauxite, gypsum, and magnesite and breakthrough characteristics of their composite filter. J. Fluor. Chem. 132, 529–535.
Tripathy, S.S., Raichur, A.M., 2008. Enhanced adsorption capacity of activated alumina by impregnation with alum for removal of As(V) from water. Chem. Eng. J. 138, 179–186.
Tsai, S.M., Wang, T.N., Ko, Y.C., 1999. Mortality for certain diseases in areas with high levels of arsenic in drinking water. Arch. Environ. Health 54, 186–193.
Tseng, C.-H., Chong, C.-K., Chen, C.-J., Tai, T.-Y., 1996. Dose-response relationship between peripheral vascular disease and ingested inorganic arsenic among residents in blackfoot disease endemic villages in Taiwan. Atherosclerosis 120, 125–133.

Viswanathan, N., Sairam Sundaram, C., Meenakshi, S., 2009. Development of multifunctional chitosan beads for fluoride removal. J. Hazard. Mater. 167, 325–331.
Organization, W.H., WHO, 2006. Guidelines for Drinking-water Quality–first Addendum to Third Edition, vol. 1. WHO Press, Switzerland. ISBN 92, 154696.
Yazdani, M., Tuudjarvi, T., Bhatnagar, A., Vahala, R., 2016. Adsorptive removal of arsenic(V) from aqueous phase by feldspars: kinetics, mechanism, and thermodynamic aspects of adsorption. J. Mol. Liq. 214, 149–156.
Zha, F., Huang, W.Y., Wang, J.Y., Chang, Y., Ding, J., Ma, J., 2013. Kinetic and thermodynamic aspects of arsenate adsorption on aluminum oxide modified palygorskite nanocomposites. Chem. Eng. J. 215, 579–585.
Zhang, W., Singh, P., Paling, E., Delides, S., 2004. Arsenic removal from contaminated water by natural iron ores. Miner. Eng. 17, 517–524.
Zhang, G.S., Qu, J.H., Liu, H.J., Liu, R.P., Li, G.T., 2007. Removal mechanism of As(III) by a novel Fe-Mn binary oxide adsorbent: oxidation and sorption. Environ. Sci. Technol. 41, 4613–4619.